European Journal of Immunology

WILEY-VCH

European Journal of Immunology
Basic • Clinical • Translational

UPDATE OPEN ACCESS

Optimising Recovery of Hepatic Regulatory T Cells: A Practical Guide Using ARTC2 Blockade

Caitlin Abbott[1] | Violette Mouro[1,2] | Chiara Perucchini[2] | Chiara Vespari[1,2] | Matteo Iannacone[1,2]

[1]Division of Immunology, Transplantation, and Infectious Diseases, IRCCS San Raffaele Scientific Institute, Milan, Italy | [2]Vita-Salute San Raffaele University, Milan, Italy

Correspondence: Matteo Iannacone (iannacone.matteo@hsr.it)

Received: 4 July 2025 | **Revised:** 23 October 2025 | **Accepted:** 3 November 2025

Tissue-resident Treg cells in nonlymphoid sites are cells that exert critical functions in situ, including maintaining local tolerance, promoting tissue repair [1], regulating insulin sensitivity [2], and preserving stem cell niches [3]. Nonetheless, these cells remain less well characterized due to technical challenges in their isolation and analysis, particularly within the liver compartment.

To study these populations effectively, isolation protocols that preserve both their viability and native phenotypic characteristics are required. Although standardized flow cytometry guidelines exist for isolating Treg cells from various tissues [4], we are providing an update to existing protocols that preserve both their viability and native phenotypic characteristics addressing underappreciated variables: (1) the inflammatory status of the tissue, and (2) the specific Treg subset of interest, whether activated effector-like (eTreg) or less activated (CD44^{mid}Treg).

Treg cells, along with other liver-resident lymphocytes such as natural killer T (NKT) and tissue-resident memory (Trm) cells, express the purinergic receptor P2RX7 [5, 6], which can be activated in an NAD$^+$-dependent ARTC2-catalyzed manner during tissue digestion, leading to cell death and reduced cell yield [7]. The anti-ARTC2 nanobody (S+16a), also known as the Treg protect reagent, blocks this pathway by preventing ARTC2-mediated ADP-ribosylation of P2RX7 [8]. However, the precise benefits of S+16a for different hepatic Treg subsets, particularly under homeostatic versus inflammatory conditions, remain incompletely defined.

To assess the impact of ARTC2 inhibition on hepatic Treg subsets at steady state, mice were treated intravenously with the anti-ARTC2 nanobody (S+16a), and intrahepatic Treg anlaysed [9]; effector Tregs (eTreg) cells were defined as CD44^{hi}, and less activated Treg (CD44^{mid}Treg) (Figure S1). The frequency of the CD44^{mid}Treg subset among CD4$^+$ T cells was similar in treated and untreated mice, while their total number per gram of liver was significantly increased upon S+16a administration (Figure 1A,B). S+16a treatment reduced the frequency of eTreg cells as a proportion of activated CD4$^+$ T cells in the liver; in contrast, the absolute number remained unchanged (Figure 1A,C). This discrepancy between percentage and cell number in the eTreg subset can be explained by the increased recovery of activated hepatic CD4$^+$ T cells with S+16a treatment (Figure S2A,D).

To determine whether S+16a also influenced Treg phenotype, we quantified the expression of key markers associated with Treg cell activation, proliferation, and function, including CD25, ICOS, Ki-67, PD-1, Nrp1, RORγt, ST2, and T-bet, by flow cytometry (Figure 1D–G; Figures S3 and S4). Phenotypically, the CD44^{mid}Treg cells from S+16a-treated mice displayed a significant increase in the proportion of CD25$^+$ cells as well as an increased level of CD25 expression (Figure 1D,E). Conversely, for eTreg cells, S+16a had minimal impact: a modest decrease in Ki-67$^+$ cells was observed by percentage, and no consistent changes were detected in other markers (Figure 1F,G; Figures S3 and S4).

Abbreviations: ARTC2, ADP-ribosyltransferase; eTreg, effector-like Treg; ICOS, inducible T cell co-stimulator; NAD, nicotinamide adenine dinucleotide; NKT cells, natural killer T; Nrp1, neuropilin 1; P2RX7, purinergic receptor 7; PD-1, programmed cell death protein 1; RORγt, retinoic acid-related orphan receptor gamma; ST2, IL-33 receptor; Tbet, Tbox transcription factor Tbx21; Treg, T regulatory; Trm, tissue-resident memory.

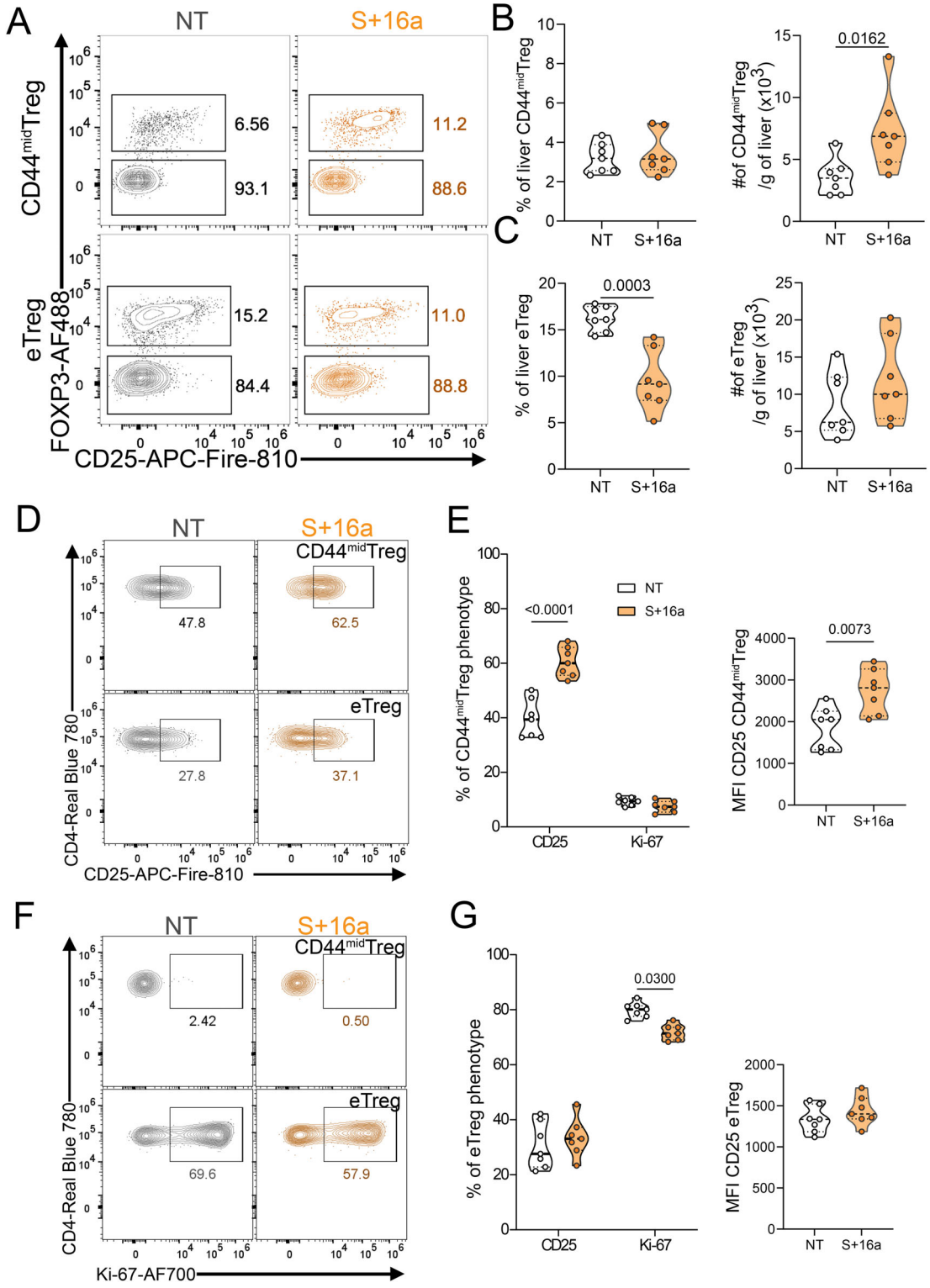

FIGURE 1 | S+16a nanobody increases total Treg yield and specifically preserves liver CD44^{mid}Treg phenotypes in the absence of inflammation. Mice were not treated (NT) or injected with S+16a. (A) Representative flow cytometry showing intrahepatic lymphocytes pregated on CD3^{+}CD4^{+}T cells to identify CD44^{hi}(eTreg) and less-activated CD44^{mid}Treg cells with S+16a or NT. (B) The percentage of liver CD44^{mid}Treg of CD4^{+}T cells (left) and the number of CD44^{mid}Treg /g of liver (right). (C) The percentage of eTreg of CD4^{+} T cells (left), and the number of eTreg/g of liver (right). Representative flow cytometry displaying D) CD25 and F) Ki-67 expression by CD44^{mid}Treg (top) and eTreg (bottom) with NT or S+16a. (E) The frequency of CD25 and Ki-67 expression by liver CD44^{mid}Treg (left) and mean fluorescence intensity (MFI) of CD25 on CD44^{mid}Treg (right). (G) The frequency of CD25 and Ki-67 expression by eTreg (left) and MFI of CD25 on eTreg (right) with NT or S+16a. Data shown as violin plots with each point representing an individual biological replicate with NT ($n = 7$), and S+16a ($n = 7$) pooled from two independent experiments. Statistics analyzed using an unpaired Student's *t*-test (B, C, E, G), or two-way ANOVA with Šidák correction (E, G). Significant *p*-values are indicated above ($p < 0.05$).

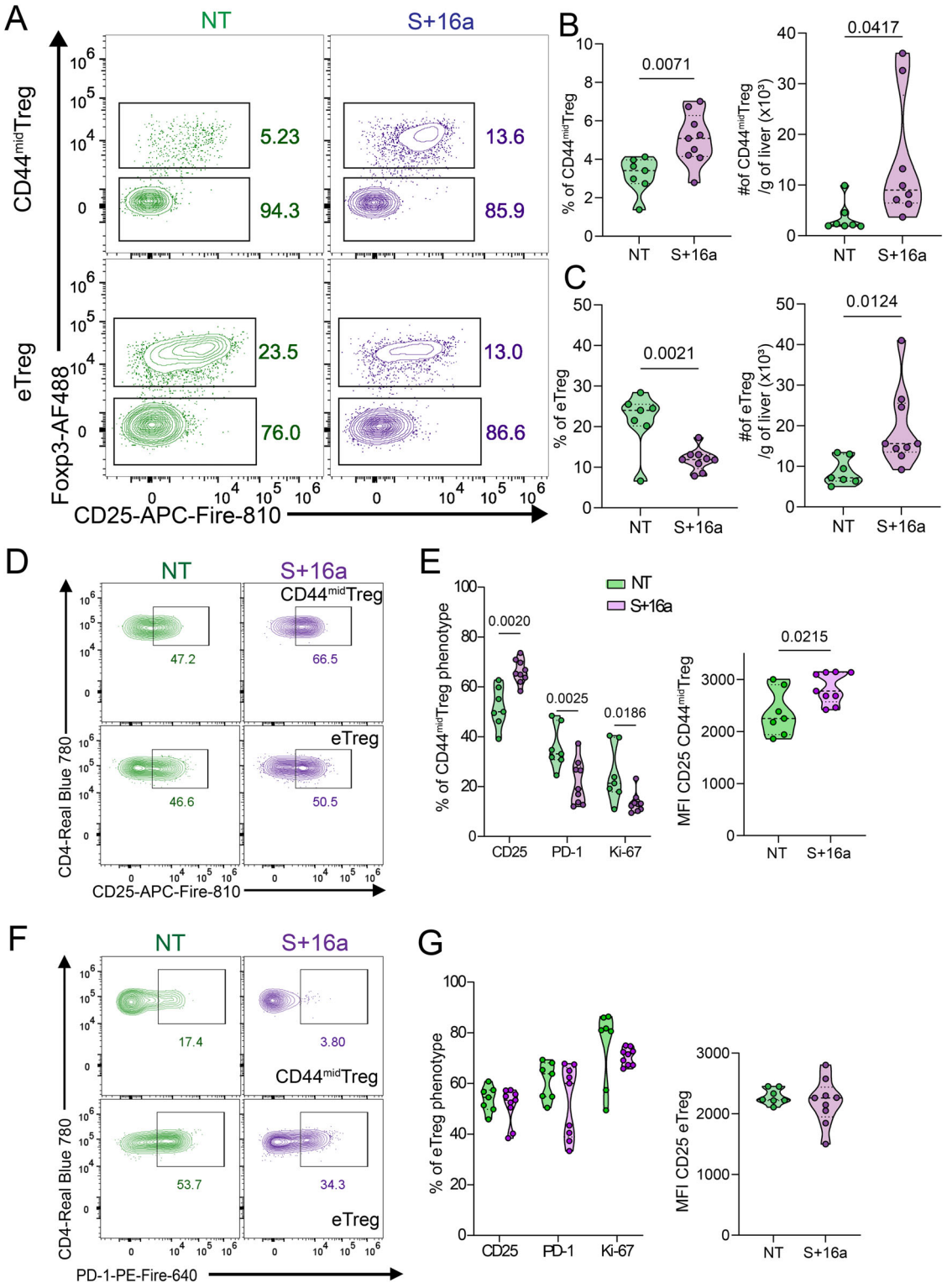

FIGURE 2 | During liver inflammation, S+16a has a greater impact on total hepatic Treg recovery and is particularly critical for recovery of CD44midTreg. Mice were treated with LPS i.p and after 24 h were either NT or injected with S+16a. (A) Representative flow cytometry showing CD44^{mid}Treg or CD44^{hi}eTreg cells with NT or S+16a. (B) The percentage of liver CD44^{mid}Treg of CD4^{+}T cells (left) and the number of CD44^{mid}Treg/g of liver (right). (C) The percentage of liver eTreg of CD4^{+}T cells (left) and the number of eTreg/g of liver (right). Representative flow cytometry of (D) CD25 expression and (F) PD-1 expression by CD44^{mid}Treg and eTreg with NT or S+16a. (E) The frequency of CD25, PD-1, and Ki-67 expression by liver CD44^{mid}Treg (left) and MFI of CD25 for liver CD44^{mid}Treg (right) with NT or S+16a. (G) The frequency of CD25, PD-1, and Ki-67 expression by eTreg (left) and MFI of CD25 for eTreg (right) with NT or S+16a. Data shown as violin plots with each point representing an individual biological replicate with NT ($n = 7$), and S+16a ($n = 9$), pooled from two independent experiments. Statistics analyzed using an unpaired Student's t-test (B, C), two-way ANOVA with Šidák correction (E, G). Significant p-values are indicated above ($p < 0.05$).

To determine whether the effects of ARTC2 inhibition extend to inflammatory conditions, mice were treated intraperitoneally with lipopolysaccharide to induce systemic inflammation with hepatic involvement [10]. Under inflammatory conditions, CD44^{mid}Treg cells increased both in frequency and absolute number following S+16a treatment (Figure 2A,B), indicating enhanced recovery of this subset. In contrast, the frequency of eTreg cells among CD4$^+$ T cells was significantly decreased in S+16a-treated mice (Figure 2A,C), despite a marked increase in their absolute number per gram of liver (Figure 2C). This apparent discrepancy reflected an overall expansion of the CD4$^+$ T cell pool, including activated cells, upon S+16a treatment, which lowered the relative frequency of the eTreg subset within the CD4$^+$ T cell compartment (Figure S2A,C,D).

We next examined whether S+16a influenced the phenotypic profile of Treg cells under inflammatory conditions. In CD44^{mid}Treg cells, S+16a treatment resulted in a notable increase in the proportion of CD25$^+$ and a decrease in the frequency of both PD-1$^+$ and Ki-67$^+$ cells (Figure 2D–F; Figure S4). Moreover, the level of CD25 expression was significantly increased in CD44^{mid}Treg cells (Figure 2D,E).

In eTreg cells, no significant differences in marker expression were observed by percentage (Figure 2D,F,G; Figures S5 and S6), although absolute numbers of total eTreg cells increased, in line with overall higher CD4$^+$ T cell recovery. This suggests that ARTC2 blockade boosts eTreg cell yield without significantly skewing their phenotype. However, unlike the eTreg subset, CD44^{mid}Treg cells undergo a phenotypic shift in the absence of ARTC2 blockade, characterized by reduced CD25 expression and increased Ki-67 and PD-1 expression.

Together, these results demonstrate that S+16a treatment significantly enhances the yield of both eTreg and CD44^{mid}Treg subsets from the inflamed liver. While eTreg cell phenotype remains largely unaffected, CD44^{mid}Treg cell recovery and phenotypic integrity, particularly the representation of less activated subsets, are substantially improved. Thus, ARTC2 blockade is especially valuable for applications requiring high-fidelity recovery of CD44^{mid}Treg cells, such as transcriptomic or epigenetic profiling, and for maximizing overall Treg cell yield in inflammatory settings.

Author Contributions

Experimental design and execution: Caitlin Abbott, Chiara Perucchini, and Violette Mouro. Data analysis: Caitlin Abbott. Funding and project supervision: Matteo Iannacone. Manuscript writing and revision: Caitlin Abbott, Violette Mouro, Chiara Vespari, and Chiara Perucchini.

Funding

M. I. is supported by the ERC advanced Grant 101141363, AIRC grants 30520 and 22737, the MRC Developmental Pathway Funding Scheme MR/Y019466/1, and Italian Ministry for University and research grants FIS-2023-00745, Pe00000007(INF-ACT), and PRIN 2022FMESXl. C. A. is supported by the European Commission with an MSCA-funded postdoctoral fellowship.

Conflicts of Interest

The authors declare no conflicts of interest.

Data Availability Statement

The data supporting the findings of this study are openly available in Zenodo at doi:10.5281/zenodo.17098563.

Peer Review

The peer review history for this article is available at https://publons.com/publon/10.1002/eji.70095.

References

1. T. M. Savage, K. T. Fortson, K. De Los Santos-Alexis, et al., "Amphiregulin From Regulatory T Cells Promotes Liver Fibrosis and Insulin Resistance in Non-Alcoholic Steatohepatitis," *Immunity* (2024): 303–318.e6, https://doi.org/10.1016/j.immuni.2024.01.009.

2. A. Vasanthakumar, D. Chisanga, J. Blume, et al., "Sex-specific Adipose Tissue Imprinting of Regulatory T Cells," *Nature* 579 (2020): 581–585, https://doi.org/10.1038/s41586-020-2040-3.

3. Z. Liu, X. Hu, Y. Liang, et al., "Glucocorticoid Signaling and Regulatory T Cells Cooperate to Maintain the Hair-Follicle Stem-Cell Niche," *Nature Immunology* 23 (2022): 1086–1097, https://doi.org/10.1038/s41590-022-01244-9.

4. A. Cossarizza, H. D. Chang, A. Radbruch, et al., "Guidelines for the Use of Flow Cytometry and Cell Sorting in Immunological Studies (Third Edition)," *European Journal of Immunology* 51 (2021): 2708–3145, https://doi.org/10.1002/eji.202170126.

5. H. Borges Da Silva, L. K. Beura, H. Wang, et al., "The Purinergic Receptor P2RX7 Directs Metabolic Fitness of Long-Lived Memory CD8+ T Cells," *Nature* 559 (2018): 264–268, https://doi.org/10.1038/s41586-018-0282-0.

6. H. Borges da Silva, H. Wang, L. J. Qian, K. A. Hogquist, and S. C. Jameson, "ARTC2.2/P2RX7 Signaling During Cell Isolation Distorts Function and Quantification of Tissue-Resident CD8+ T Cell and Invariant NKT Subsets," *Journal of Immunology* 202 (2019): 2153–2163, https://doi.org/10.4049/jimmunol.1801613.

7. S. Hubert, B. Rissiek, K. Klages, et al., "Extracellular NAD+ Shapes the Foxp3+ Regulatory T Cell Compartment Through the ART2–P2X7 Pathway," *Journal of Experimental Medicine* 207 (2010): 2561–2568, https://doi.org/10.1084/jem.20091154.

8. F. Koch-Nolte, J. Reyelt, B. Schößow, et al., "Single Domain Antibodies from llama Effectively and Specifically Block T Cell Ecto-ADP-Ribosyltransferase ART2.2 in Vivo," *Faseb Journal* 21 (2007): 3490–3498, https://doi.org/10.1096/fj.07-8661com.

9. S. Spath, F. Roan, S. R. Presnell, B. Höllbacher, and S. F. Ziegler, "Profiling of Tregs Across Tissues Reveals Plasticity in ST2 Expression and Hierarchies in Tissue-specific Phenotypes," *Iscience* 25 (2022): 104998, https://doi.org/10.1016/j.isci.2022.104998.

10. K. Hamesch, E. Borkham-Kamphorst, P. Strnad, and R. Weiskirchen, "Lipopolysaccharide-Induced Inflammatory Liver Injury in Mice," *Laboratory Animals* 49 (2015): 37–46, https://doi.org/10.1177/0023677215570087.

Supporting Information

Additional supporting information can be found online in the Supporting Information section.

Supporting File: eji70095-sup-0001-SuppMat.pdf